## Response to Reviewer 2

Firstly, we thank the reviewer for taking the time to evaluate our manuscript and for providing detailed comments and constructive suggestions. We greatly appreciate the reviewer's effort, which has helped us to improve the clarity, rigor, and overall quality of the manuscript. In the revised manuscript, Reviewer 2's comments are shown in blue, with our responses provided directly below each comment.

**1.** ***It is unclear what resolution is used in the application of the TSEB model. The 15 cm resolution is very high and it is not clear how it can be used to define the inputs to TSEB. This needs to be clearly discussed.***

We appreciate this comment and agree that the original manuscript did not clearly state the spatial resolution used in the UAV TSEB implementation. We have revised to clarify that TSEB was run on a 15 cm model grid, which corresponds to the finest common resolution supported by the UAV thermal and LiDAR products (according to flight parameters) used in our study.

This fine resolution was selected to improve the derivation of TSEB inputs by minimizing mixed soil and vegetation pixels, particularly during early growth stages and partial canopy cover. At 15 cm, vegetation and soil fractions (and associated LST and canopy structure metrics) can be more robustly discriminated, improving retrieval of key drivers such as LST, LAI, and the green fraction of LAI. Similar UAV TSEB studies have commonly applied sub-meter resolutions for this purpose (e.g., Hoffmann et al., 2016; Gómez-Candón et al., 2021; Gao et al., 2023). This clarification has been added to the revised manuscript.

***Paper Improvement:***

- Clarified the high-resolution rationale in the Introduction and Methods.

**2.** ***Only compare ET and not the other energy balance components nor do they mention how they dealt with energy balance closure. Comparison with closed or unclosed H and LE should be discussed. Furthermore, an X-Y scatter plot comparing all 4 components for each crop type would be very helpful to the reader.***

We thank the reviewer for this important comment and agree that evaluation of TSEB performance should include the full surface energy balance components (Rn, H, G, and LE), not only ET/LE. Our original focus was on ET because it is the primary variable for water-use monitoring and several recent UAV TSEB studies have validated LE/ET alone (Tunca, 2023a; de Lima et al., 2024; Pintér & Nagy, 2022). However, we agree that assessing the full set of energy fluxes improves transparency.

We have therefore updated the revised manuscript to include direct comparisons of modeled versus EC-derived Rn, H, and G, and we now present validation results using both open EC fluxes and closed energy-balance H and LE fluxes. Energy balance closure was performed using a Bowen-ratio-preserving correction following Twine et al. (2000), consistent with approaches commonly used in comparable UAV TSEB studies (e.g., Hoffmann et al., 2016; Brenner et al., 2017, 2018; Wei et al., 2023; Gao et al., 2023). We initially emphasized comparisons against open EC fluxes to avoid introducing closure-related assumptions (Mokhtari et al., 2021; Nassar et al., 2021), but now provide both open and closed comparisons for completeness.

Following the reviewer's suggestion, we also added X–Y scatter plots for all four flux components (Rn, H, G, and LE) for each crop type and provide corresponding performance statistics (included in the revised manuscript in a supplementary table).

***Paper Improvement:***

- Added Rn/H/G/LE scatter plots for each crop. These new figures are included in the revised manuscript and are also provided in the response supplement ("New Figures"), Figures R1 and R3.
- Included comparisons against both open and closed energy balance EC fluxes and expanded the discussion of EC closure implications.
- Included the RMSE and $R^2$ bar graph figures comparing UAV TSEB ET with EC ET from both open and closed energy balances. The figures can be seen in "New Figures" at the end of this document and labeled Figure R2 and R4.

### 3. *There are also several fractional cover terms discussed but is confusing to the reader which ones are applied under the different crop conditions (e.g., pre and post senescence).*

We thank the reviewer for highlighting this point. We agree that several "fractional cover" terms were described in the original manuscript and that it was not sufficiently clear which ones were applied under different crop conditions (pre- vs post-senescence). In addition, some terminology in Table 1 / Appendix was previously ambiguous (and in places incorrectly labeled), which contributed to confusion. To remove ambiguity, we have revised the text to consistently distinguish and define the following terms:

- **FVC (fractional vegetation cover):** nadir-view vegetation cover derived from multispectral imagery (NDVI thresholding). In our workflow, FVC is used only as an intermediate variable to derive GAI.
- **$f_c$ (TSEB canopy fractional cover):** the internal view-angle-dependent canopy fraction used in pyTSEB for radiative partitioning between canopy and soil; it is computed internally from LAI and canopy parameters and is not equivalent to the FVC we used to derive GAI.

- **$f_g$ (fraction of green LAI):** the fraction of LAI that is photosynthetically active ("green"), used to account for senescence and avoid treating senescent canopy structure as fully transpiring.

We also clarified the pre-/post-senescence implementation: prior to senescence, $f_g$=1), while during senescence $f_g$ decreases and is quantified using combined multispectral and LiDAR information ($f_g$=GAI/PAI). This clarification and consistent notation and terminology have been applied throughout the revised manuscript (Table 1, Fig. 4, and Appendix text/equations).

***Paper improvement:***

- We revised Table 1, Fig. 4, and Appendix equations/text to consistently distinguish MS derived FVC, internal TSEB $f_c$ and green fraction $f_g$
- Added explicit clarification of pre-/post-senescence interpretation and parameterization.

### *4. With such high resolution thermal and multispectral imagery, could the authors have also used the TSEB-2T version? If not, they should provide rationale in going with TSEB-PT.*

Given the very high-resolution thermal and multispectral imagery, we did initially evaluated both TSEB-2T and TSEB-PT during the 2021 campaign. We found that TSEB-2T could slightly improve ET estimation under early-season sparse canopy conditions (e.g., sugar beet with substantial exposed soil), where separating soil and canopy temperature contributions is more meaningful. However, as canopy closure increased in the season, any improvement from TSEB-2T was not consistent and in some cases performance degraded relative to TSEB-PT.

Therefore, we selected TSEB-PT as the primary configuration because it appeared it provided more stable and robust performance across crop types and phenological stages in our study, while still allowing physically constrained partitioning of canopy and soil fluxes using composite radiometric temperature and LAI radiative partitioning. This choice is also consistent with comparative studies showing that performance differences between TSEB-2T and TSEB-PT can be marginal and crop-dependent (e.g., Nieto et al., 2019; Guzinski et al., 2020; Gao et al., 2023).

Nevertheless, we acknowledge that TSEB-2T can be advantageous for sparse/discontinuous canopies with persistent soil exposure (e.g., vineyards/orchards), where soil contributions dominate and component temperature separation is more reliable, as demonstrated in several UAV TSEB vineyard studies. We have added this rationale and supporting references to the revised manuscript.

***Paper improvement:***

- Added to the introduction and discussion with mentioned citations about possible improvements with TSEB-2T with large and/or consistent soil exposure.
- Added explanation in introduction to why TSEB-PT was chosen over TSEB-2T in this use case but that there could be benefits to using TSEB-2T in other cases.

5. ***Some of the figures should be modified for better clarity. For example, in Figure 5 the authors should consider adding a 2nd y-axis to show the difference in LST_OG and LST_TC as the temperature range from 10 to 40 C significantly suppresses differences in the plots. The figures 8 ands 10 would be more useful to the reader if they were shown as scatter plots (2 x 3 separating the two LST inputs versus EC observations and for LAI a 3x3 for the three LAI/fg estimates) and distinguishing with symbols pre and post senescence. Also for both current figures 8 and 10 the symbols for LST=LST_OG and LAI=GAI, fg=1 are very faint and hard to see. Plus, the vertical dashed lines I believe indicate pre and post crop senescence but are not mentioned in the figure captions and should be a darker color (black?) so is easily visible to the reader. Finally, there are unexplained dashed light blue lines for the potato plots which are not described. However, I believe scatter plots would be much more useful to the reader and easier to evaluate differences with the EC data as scatter plots. On the other hand, I like the way the authors show the difference statistics for the different model output in figures 9 and 11. In Figure 13, the figures have an insert with a blue circle…seems out of place and not explained.***

- **Figure 5:** Added a second y-axis showing ΔLST (LST_TC – LST_OG), as suggested, to better highlight the magnitude of the thermal correction. The revised figure is provided in the response supplement ("New Figures", Fig. R6).
- **Figures 8 & 10:** improved readability of previously faint cases (e.g., LST=LST_OG and LAI=GAI, $f_g$=1) by increasing font/marker visibility and contrast.
- We agree to that the use of scatter plots for all the fluxes is a good addition and will add something similar to the suggestions. However, we propose to have a 2x3 figures separating comparison with open and closed EC while keeping different LST inputs in the same graph to see the impact on the change in flux amounts. The same is applied of the LAI methods. We alos distinguish between pre- and post senescence with different shading. These figures can be seen at the end of this document (attached) Figure R1 & R3.

- **Symbol visibility and explanations:** Increased line widths and marker sizes, improved contrast, changed senescence divider line markers to black, and expanded figure captions / figure index to explicitly describe all plot elements.
- **Blue boxes (Figure 13):** Clarified that the blue boxes indicate the zoomed subset area within the agricultural field and added this explanation to the caption and figure index.

**6.** ***Under section 4.5 Practical impacts and considerations for farming practices, the authors should go the extra mile and compute daily ET using the simple approach evaluated by Cammalleri et al (2014). This approach is used and tested in many applications even with UAV data (e.g., Nassar et al. 2021). I recommend the authors make a final calculation using this approach and compare with daily ET from the EC data using their best inputs. The daily ET is more relevant to farmers and for stress perhaps they can show these daily ET maps relative to reference crop or potential ET from FAO56 to highlight the stress area.***

We agree that daily ET products are more directly relevant for irrigation management than instantaneous flux estimates. In the original manuscript, our primary focus was on evaluating the accuracy of instantaneous UAV TSEB fluxes at the time of overpass (validated against 1-hour EC fluxes) in order to isolate the impact of UAV inputs (thermal correction, LAI, and $f_g$) without introducing additional uncertainty from temporal upscaling.

Following the reviewer's recommendation, we have now included a daily ET upscaling component using the approach evaluated by Cammalleri et al. (2014), which has also been applied and tested in UAV based contexts (e.g., Nassar et al., 2021). Using our best-performing UAV TSEB configuration, we now generate daily ET estimates and directly compare them with EC daily ET, reported for both open and closed conditions.

As suggested, we additionally include a daily-scale stress proxy by presenting daily ET relative to FAO-56 reference/potential ET ($K_s$) which highlights spatial and seasonal patterns of water deficit conditions.

***Paper Improvement****:*

We added a short analysis showing how our UAV TSEB daily ET patterns align with EC ET patterns and potential ET (FAO-56), demonstrating consistency in identifying high- and low-ET zones. Added a daily-scale stress interpretation by presenting daily ET relative to FAO-56 reference/potential ET

- Added a new figure showing daily ET comparisons and the daily-scale stress proxy (daily ET / potential ET) (see “New Figures”, Fig. R5 at the next section).

## *New Paper Figures*

This document provides additional figures generated for the revision, including (i) expanded validation against open and energy-balance-closed eddy covariance (EC) fluxes for all energy balance components, (ii) sensitivity comparisons for land surface temperature (LST) and LAI/green fraction parameterizations, and (iii) daily ET upscaling and stress proxy analysis.

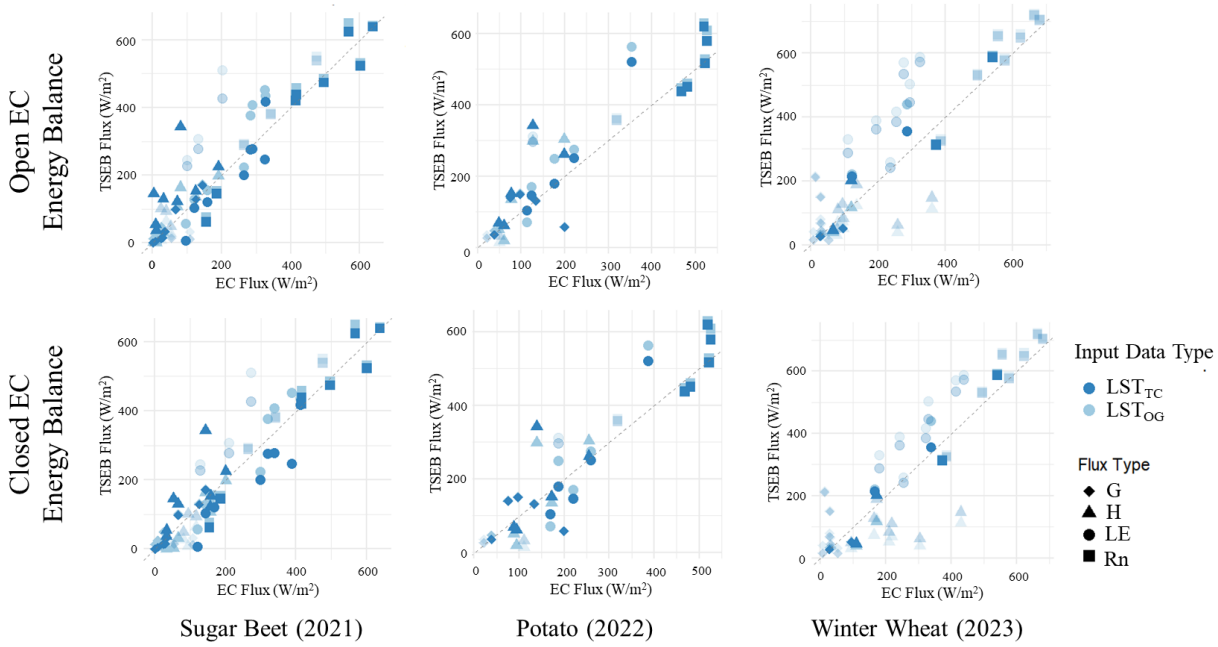


**Figure R1.** Comparison of modeled TSEB fluxes against eddy covariance (EC) flux observations for each crop season. The upper panels show comparisons using open EC energy balance fluxes, while the lower panels show comparisons using closed EC energy balance fluxes obtained with the Bowen-ratio-preserving correction. The colors indicate the two land surface temperature inputs while the shapes indicate the different fluxes. Shaded points represent observations acquired during the defined crop senescence period.

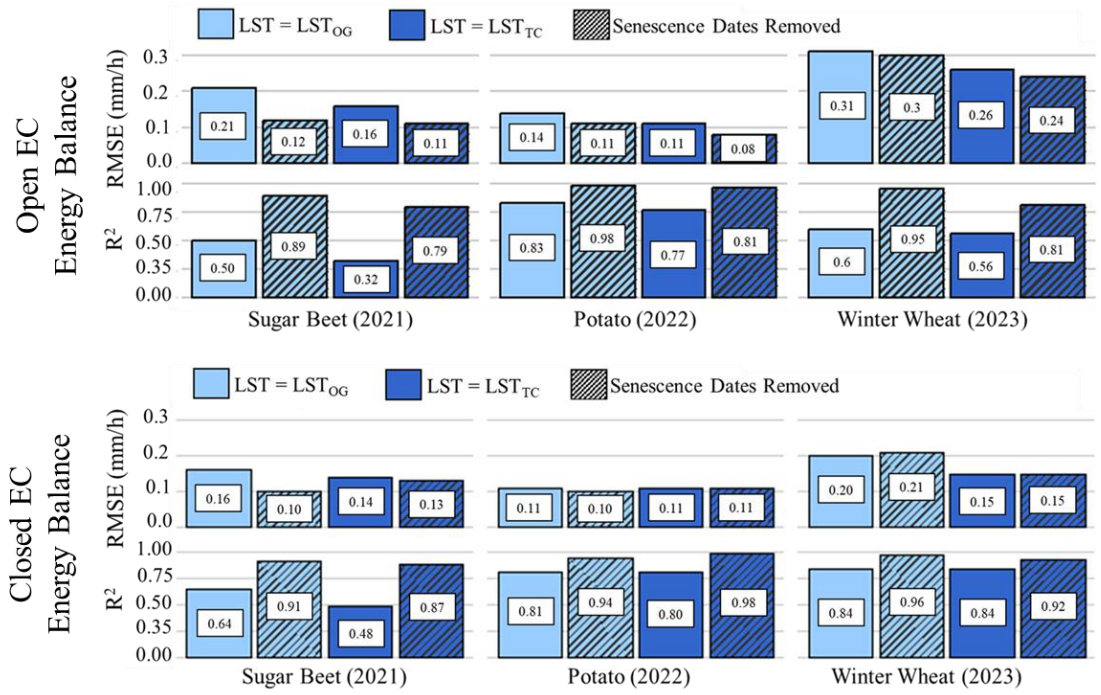


**Figure R2**. RMSE and $R^2$ between modeled TSEB-PT ET and EC derived ET, open and closed energy balances, averaged over the EC flux footprint. Two TSEB-PT model runs are compared based on land surface temperature (LST) input: original (OG) and target corrected (TC). Statistical metrics are presented for the entire growing season and excluding senescence periods, highlighting the influence of canopy condition on model performance.

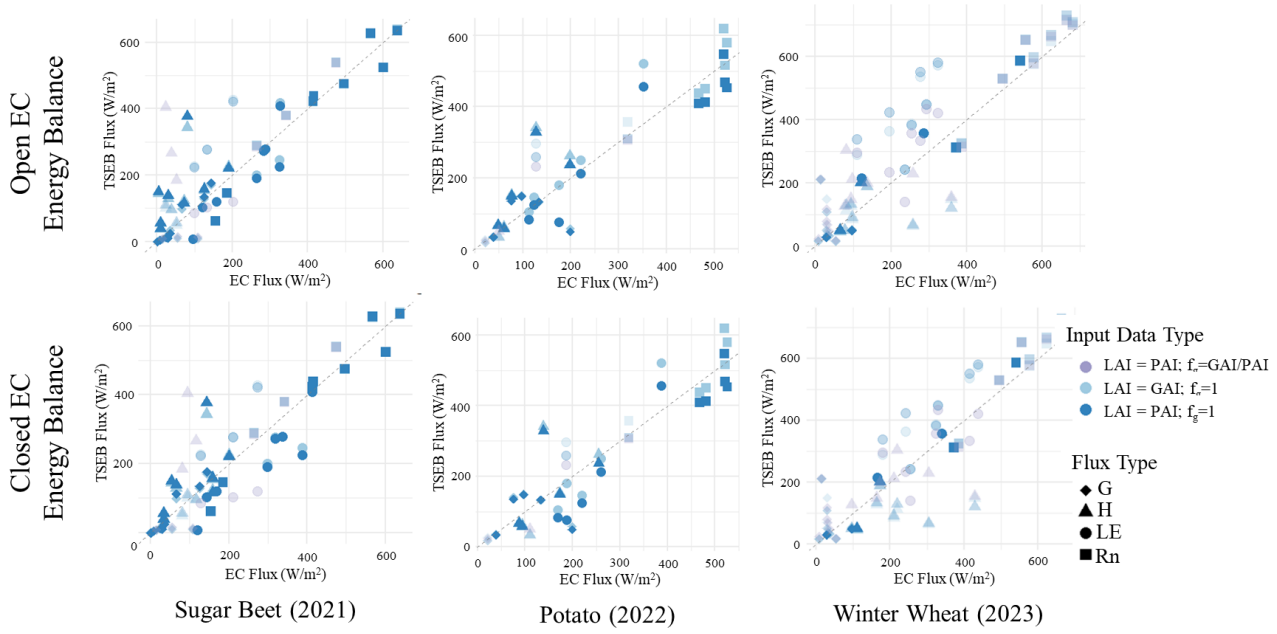


**Figure R3.** Comparison of modeled TSEB energy balance fluxes against eddy covariance (EC) observations for each crop season under different UAV derived vegetation parameter configurations (LAI inputs and fraction of green LAI). The upper panels show comparisons using open EC fluxes, while the lower panels show comparisons using closed energy balance EC fluxes obtained with a Bowen-ratio-preserving correction. Colors indicate the LAI/$f_g$ configurations, while marker shapes distinguish the individual flux components. Lighter markers represent observations acquired during the defined crop senescence period.

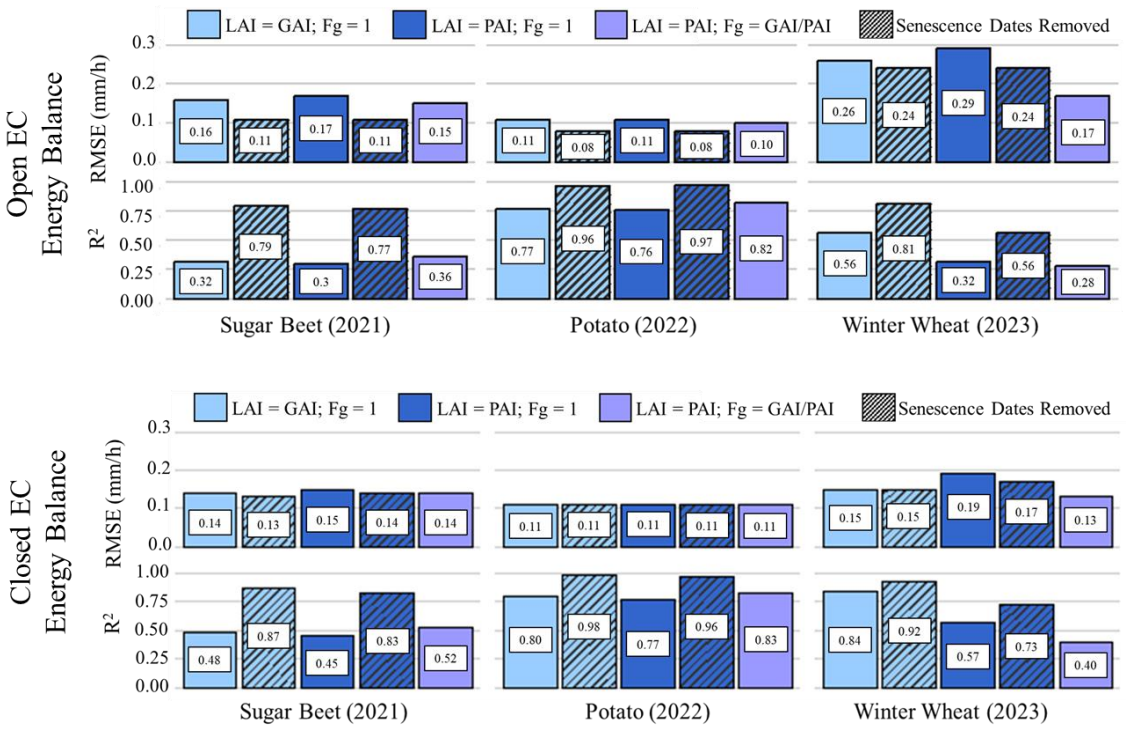


**Figure R4**. RMSE and $R^2$ between TSEB-PT modeled ET and EC derived ET, open and closed energy balances, averaged over the EC flux footprint. Two different LAI inputs were evaluated: green area index (GAI) and plant area index (PAI). Statistical metrics are shown for all campaign dates and separately for dates excluding senescence. During senescence periods, a third approach using the fraction of green LAI ($f_g$ = GAI/PAI) was also evaluated to scale transpiration according to functional canopy condition.

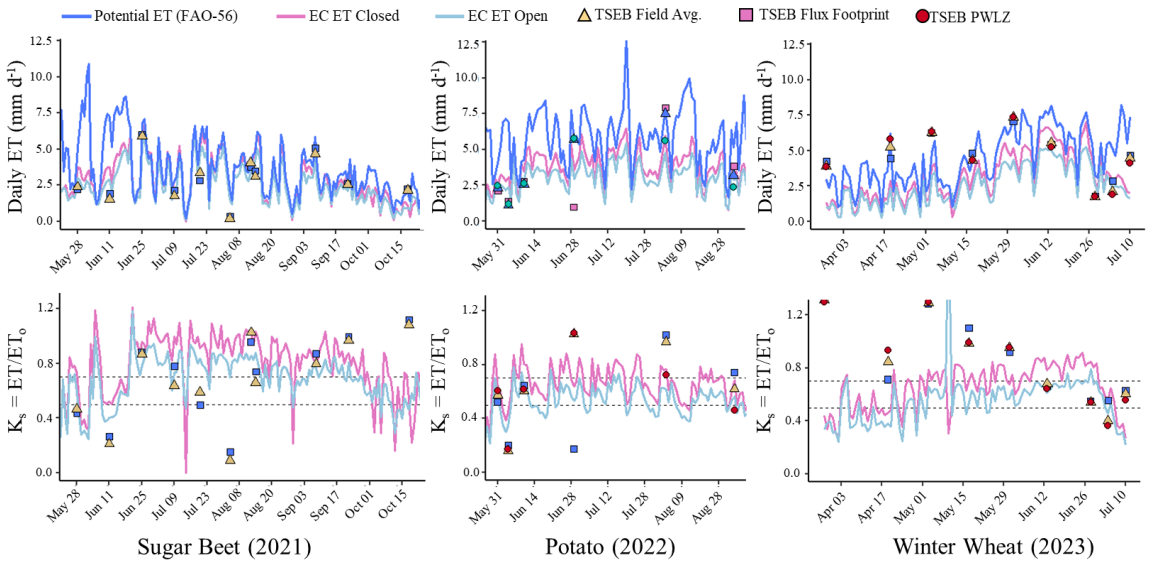


**Figure R5.** Daily evapotranspiration (ET) time series and daily-scale stress proxy derived from UAV–TSEB and EC measurements. **Top panels:** interpolated daily ET from UAV acquisition compared against EC daily ET (open and closed energy balances) and FAO-56 reference/potential ET. **Bottom panels:** corresponding relative ET stress proxy ($K_s$) computed as the ratio of daily actual ET to FAO-56 reference/potential ET, illustrating seasonal development of water deficit conditions across crops. Horizontal dashed lines represent 0.7 possible water stress and 0.5 likely water stress compared to atmospheric demand. The different shapes depict different spatial domains of pixel averages from the UAV instantaneous UAV ET that is then upscaled to daily it with including TSEB field average, the flux footprint weighted average, and the average within the potential water limitation zones (PWLZ) from figures 14 and 15.

## *References:*


Brenner, C., Thiem, C. E., Wizemann, H.-D., Bernhardt, M., & Schulz, K. (2017). Estimating spatially distributed turbulent heat fluxes from high-resolution thermal imagery acquired with a UAV system. International Journal of Remote Sensing, 38(8–10), 3003–3026. https://doi.org/10.1080/01431161.2017.1280202

Brenner, C., Zeeman, M., Bernhardt, M., & Schulz, K. (2018). Estimation of evapotranspiration of temperate grassland based on high-resolution thermal and visible range imagery from unmanned aerial systems. International Journal of Remote Sensing, 39(15–16), 5141–5174.

Cammalleri, C., Anderson, M.C., Kustas, W.P. (2014). Upscaling of evapotranspiration fluxes from instantaneous to daytime scales for thermal remote sensing applications. Hydrol. Earth Syst. Sci. 18, 1885–1894

de Lima, G. S. A., Ferreira, M. E., Sales, J. C., de Souza Passos, J., Maggiotto, S. R., Madari, B. E., de Melo Carvalho, M. T., & de Almeida Machado, P. L. O. (2024). Evapotranspiration measurements in pasture, crops, and native Brazilian Cerrado based on UAV-borne multispectral sensor. Environmental Monitoring and Assessment, 196(11), 1105. https://doi.org/10.1007/s10661-024-13224-7

Gao, R., Torres-Rua, A. F., Nieto, H., Zahn, E., Hipps, L., Kustas, W. P., Alsina, M. M., Bambach, N., Castro, S. J., Prueger, J. H., Alfieri, J., McKee, L. G., White, W. A., Gao, F., McElrone, A. J., Anderson, M., Knipper, K., Coopmans, C., Gowing, I., … Dokoozlian, N. (2023). ET Partitioning Assessment Using the TSEB Model and sUAS Information across California Central Valley Vineyards. Remote Sensing, 15(3), 756.

Gómez-Candón, D., Bellvert, J., & Royo, C. (2021). Performance of the Two-Source Energy Balance (TSEB) Model as a Tool for Monitoring the Response of Durum Wheat to Drought by High-Throughput Field Phenotyping. Frontiers in Plant Science, 12.

Guzinski, R., Nieto, H., Sandholt, I., & Karamitilios, G. (2020). Modelling High-Resolution Actual Evapotranspiration through Sentinel-2 and Sentinel-3 Data Fusion. Remote Sensing, 12(9), Article 9. https://doi.org/10.3390/rs12091433

Hoffmann, H., Nieto, H., Jensen, R., Guzinski, R., Zarco-Tejada, P., & Friborg, T. (2016). Estimating evaporation with thermal UAV data and two-source energy balance models. Hydrology and Earth System Sciences, 20(2), 697–713.

Mokhtari, A., Ahmadi, A., Daccache, A., & Drechsler, K. (2021). Actual Evapotranspiration from UAV Images: A Multi-Sensor Data Fusion Approach. Remote Sensing, 13(12), Article 12. https://doi.org/10.3390/rs13122315

Nassar, A., Torres-Rua, A., Kustas, W., Alfieri, J., Hipps, L., Prueger, J., Nieto, H., Alsina, M. M., White, W., McKee, L., Coopmans, C., Sanchez, L., & Dokoozlian, N. (2021). Assessing Daily Evapotranspiration Methodologies from One-Time-of-Day sUAS and EC Information in the GRAPEX Project. Remote Sensing, 13(15), Article 15. https://doi.org/10.3390/rs13152887

Nieto, H., Kustas, W. P., Torres-Rúa, A., Alfieri, J. G., Gao, F., Anderson, M. C., White, W. A., Song, L., Alsina, M. del M., Prueger, J. H., McKee, M., Elarab, M., & McKee, L. G. (2019). Evaluation of TSEB turbulent fluxes using different methods for the retrieval of soil and canopy component temperatures from UAV thermal and multispectral imagery. Irrigation Science, 37(3), 389–406.